

The abrasive flow machining simulation of common rail tube holes based on FLUENT

Lifeng Zhu^{1, a}, Kai Wang^{2, 3, b}, Huan Wu^{3, c}, Dong Xiu^{3, d}, Lizhong Sun^{3, e}

¹Changchun University of Science and Technology, Changchun 130022, China

²Jilin University State Key Laboratory of Automotive Simulation and Control, Changchun, China

³Changchun Institute of Equipment and Process, Changchun 130012, China

^a14075241@qq.com, ^b46345189@qq.com, ^c 42956512@qq.com, ^d86113066@qq.com

Keywords: common rail; Abrasive Flow Machining; FLUENT; numerical analysis

Abstract: Based on the solid - liquid two-coupling theory, Use abrasive medium viscosity-temperature characteristics related to the mathematical model, using solid - liquid two-phase solution method Mixture models and standards $k - \varepsilon$, turbulence model combining with common rail pipe hole as the research object, choose different initial temperatures and processing procedures, numerical analysis was carried out on the flow channel wall temperature and turbulent kinetic energy. Using numerical analysis software FLUENT Abrasive Flow Machining rail tube orifice structure was three-dimensional numerical analysis; obtain a steady-state pressure, dynamic pressure, velocity, turbulent kinetic energy image, to study Abrasive Flow Machining process provides a theoretical basis and technical support.

Introduction

Common rail is an important component part of the engine fuel supply system, common rail inside the tiny hole polishing and debarring has been the problem to be solved with the increase^[1].

Common rail pipe of tiny holes machining quality directly affect the atomization characteristics of the common rail pipe, oil line penetration and flow coefficient, will ultimately affect the economy, power performance and emission of the engine. Common rail parts three-dimensional model is shown in Figure 1.

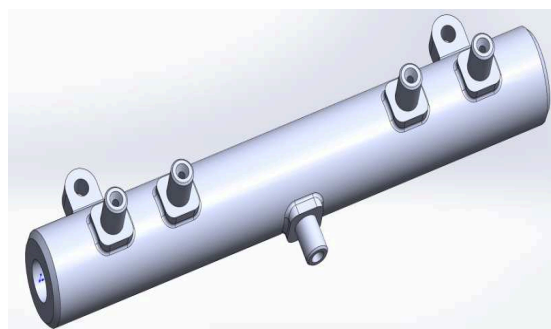


Fig. 1 Common rail parts three-dimensional map

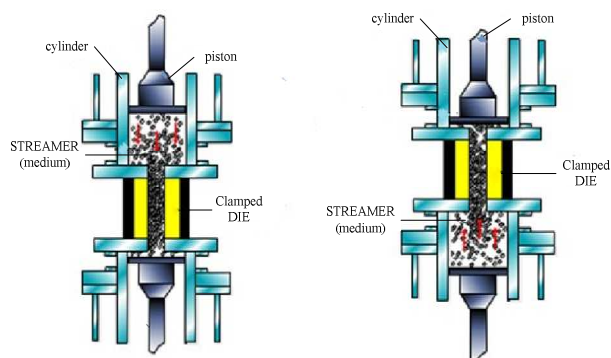


Fig. 2 Abrasive Flow Machining schematics

Common rail having high hardness, low surface roughness, in the rounded parts of the cross bore, the inner tube, and a smooth surface without burrs characteristics. Using traditional processing methods to achieve the common rail pipe cross hole deburring and rounding is its difficulty, Abrasive Flow Machining technology appears to solve this problem provides an effective way^[2, 3]. Abrasive flow machining principle is shown in figure 2.

Abrasive Flow Machining technology is achieved by a viscoelastic body containing abrasive soft abrasive media, under pressure reciprocating flow through the parts to be machined surfaces to achieve Finishing. We use abrasive stream as a myriad of cutting tool, the workpiece surface with its hard sharp edges and corners of repeated cutting, so as to achieve a certain purpose. Any part of the stream flowing through the abrasive will be finishing, for those components in contact with the general tools are difficult to lumen, the advantages of abrasive flow machining technology is particularly prominent. When the abrasive grains uniformly and progressively to the flow path surface or edge working, can produce deburring, polishing, chamfering role^[4, 5].

1 Establish common rail mathematical model of the solid-liquid two-phase flow

Study described by Newton's laws of motion of the particles, two-phase coexist on the same point in space, their compliance with their own momentum, mass and energy transfer equation, the two phases interphase forces and shared by pressure field coupled to each other [6]. Standard $k-\varepsilon$ model turbulent kinetic energy dissipation rate and the transport equation are:

$$\frac{\partial(\rho k)}{\partial t} + \frac{\partial(\rho k u_i)}{\partial x_i} = \frac{\partial}{\partial x_j} \left[\left(\mu + \frac{\mu_t}{\sigma_k} \right) \frac{\partial k}{\partial x_j} \right] + G_k - \rho \varepsilon \quad (1)$$

$$\frac{\partial(\rho \varepsilon)}{\partial t} + \frac{\partial(\rho \varepsilon u_i)}{\partial x_i} = \frac{\partial}{\partial x_j} \left[\left(\mu + \frac{\mu_t}{\sigma_\varepsilon} \right) \frac{\partial \varepsilon}{\partial x_j} \right] + C_{1\varepsilon} G_k \frac{\varepsilon}{k} - C_{2\varepsilon} \frac{\varepsilon^2}{k} \quad (2)$$

Where, t is time, s ; $i, j = \{1, 2, 3\}$ tensor represents the subscript, $x_i = \{x_1, x_2, x_3\}$ represents the coordinates of the tensor, $u_i = \{u_1, u_2, u_3\}$ represents a velocity vector \mathbf{u} in Component 3 coordinate axis; k said turbulent kinetic energy, m^2/s^2 ; $G_k = \mu_t \left(\frac{\partial u_i}{\partial x_j} + \frac{\partial u_j}{\partial x_i} \right) \frac{\partial u_i}{\partial x_j}$ said the

average velocity gradient caused by the generation of turbulent kinetic energy k item, $kg/m \cdot s^3$; $\sigma_k = 1.0$ represents the turbulent kinetic energy K corresponding Prandtl number; $\sigma_\varepsilon = 1.3$ said dissipation rate corresponding Prandtl number; $C_{1\varepsilon} = 1.41-1.45$, $C_{2\varepsilon} = 1.91-1.92$ representation model empirical coefficients; in the formula (1), (2), and calculated as follows:

$$\mu_t = \rho C_\mu \frac{k^2}{\varepsilon} \quad (3)$$

Among them, μ_t said turbulent viscosity, $N \cdot s/m^2$;

$C_\mu = \frac{1}{4 + \sqrt{6} \cos \phi U^* k / \varepsilon}$ represents a model coefficient;

$\phi = \frac{1}{3} \cos^{-1}(\sqrt{6}W)$ represents an intermediate variable;

$W = \frac{E_{ij} E_{jk} E_{kj}}{(E_{ij} E_{ij})^{3/2}}$ represents an intermediate variable;

E represents when the average strain rate tensor modulus;

$U^* = \sqrt{E_{ij} E_{ij} + \tilde{\Omega}_{ij} \tilde{\Omega}_{ij}}$ represents an intermediate variable;

Ω_{ij} represents when both rotation rate tensor;

$\tilde{\Omega}_{ij} = \Omega_{ij} - 2\varepsilon_{ijk} \bar{\omega}_k$, $\Omega_{ij} = \bar{\Omega}_{ij} - \varepsilon_{ijk} \bar{\omega}_k$;

ω_k represents the angular velocity.

2 The simulation model establishment and parameter Settings

In the process of numerical analysis, assuming chemical dissolution or crystallization does not occur between the process medium with the particle phase; the particulate solid abrasive medium having the same pressure; granular solid abrasive media were satisfied with the conservation of momentum and energy conservation equations; the interaction between the abrasive and the particulate solid medium is realized through the drag coefficient [4, 5].

According to the data provided by the enterprise, to simulate the nozzle diameter is $\Phi 0.16\text{mm}$ common rail hole machining conditions. Using the FLUENT software GAMBIT pretreatment module of common rail pipe parts to create with the division of grid work created with the grid model. According to Abrasive Flow Machining process characteristics, choose uncoupled implicit double precision solver in FLUENT, using standard solid-liquid two-phase Mixture $k-\varepsilon$ turbulence model for numerical analysis; Abrasive Flow media carrier based main phase, the second phase is set to silicon carbide particles, the volume fraction of 0.1; select the pressure inlet boundary conditions and pressure outlet boundary conditions boundary conditions, and the rest is defined as the solid wall boundary conditions; consider the influence of gravity.

3 Simulation results and analysis

When the parameter set up, using SIMPLEC algorithm two-phase flow equation, after initializing the iterative calculations, common rail pipe holes Abrasive Flow Machining process fluid dynamics numerical analysis. After the calculation, get residuals to monitor changes in the curve shown in Figure 4.

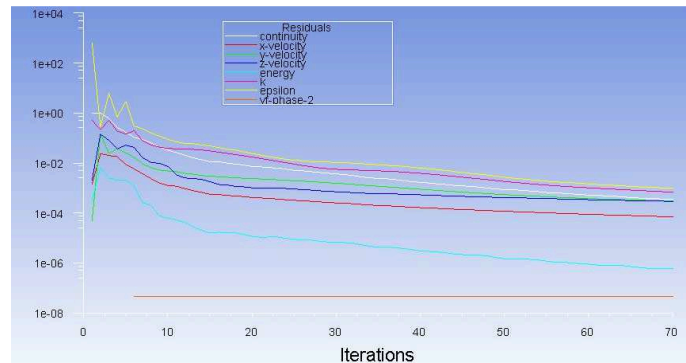
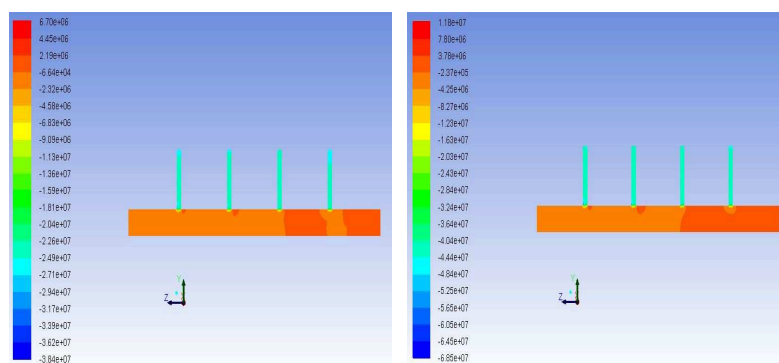


Figure 4 Residual monitoring curve

As can be seen from the residual curve, beginning at about 70 iterations convergence, indicating the model and solution design parameters set reasonable, can be satisfied with the converged solution. In order to more accurately simulate real Abrasive Flow Machining common rail hole conditions, using three-dimensional numerical simulation method of characteristics Abrasive Flow Machining rail tube numerical analysis obtained simultaneously abrasive flow machining rail tube structure all holes processing characteristics.

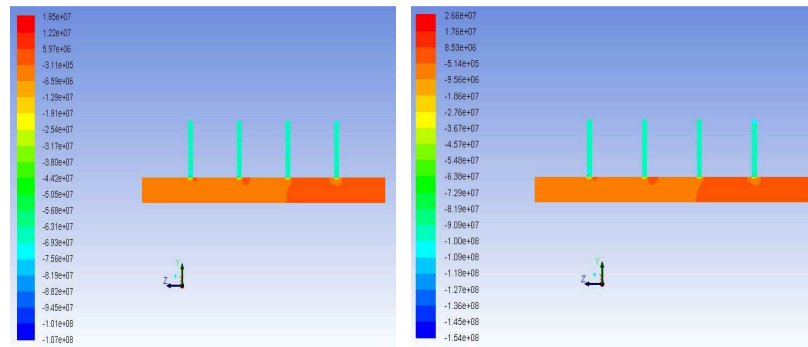
3.1 Numerical analysis of steady-state pressure

Numerical analysis methods using simulated inlet conditions at different speeds simultaneously abrasive flow machining conditions common rail all holes structure, access to the steady pressure of the image shown in Figure 5. As can be seen by observing, close to the hole in the common rail pressure showed a decreasing trend at other places within the flow channel to maintain steady pressure of the same size. Holes in the common rail pressure at steady-state pressure significantly, indicating abrasive flow where the most intense sport. Due to the common rail and rail throughout the flow channel tube orifice diameter and length difference between the larger, the difference between the force per unit area is also a great role in a larger hole in force at the common rail, common rail favor spray holes fine polishing process, to better ensure accuracy at the common rail pipe holes.



A) In and out of the speed is 30 m/s

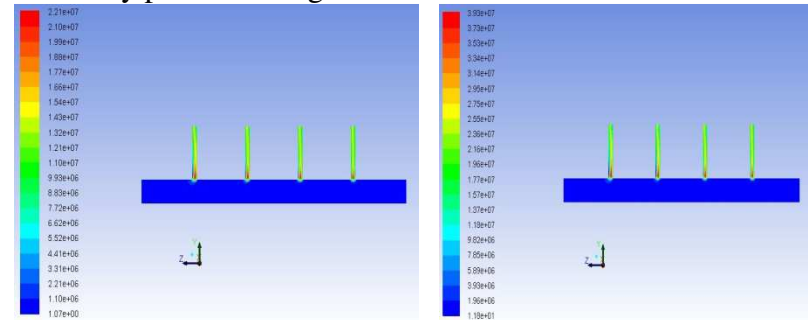
B) inlet velocity is 40 m/s



C) in and out of speed is 50 m/s

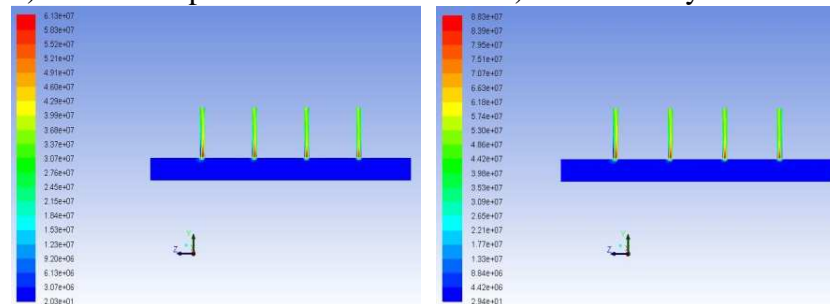
D) inlet velocity is 60 m/s

Figure 5 Steady pressure images of Entrance conditions at different speeds



a) out of the speed of 30m / s

b) inlet velocity of 40m / s



c) out of the speed of 50m / s

d) inlet velocity of 60m / s

Figure 6 Image dynamic pressure inlet conditions at different speeds

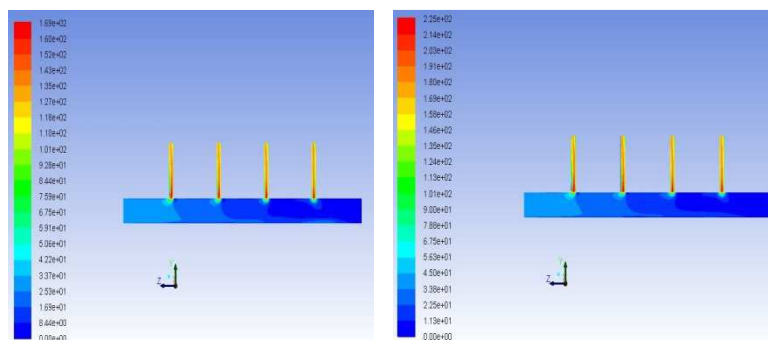
3.2 Numerical analysis of dynamic pressure

Dynamic pressure is the relative strength of indicators to measure the turbulence, is to describe the extent of the velocity changing with time and space, is reflects the relative intensity fluctuation velocity, turbulent motion characteristics describe the most important characteristic quantities.

With the increasing inlet velocity, dynamic pressure inside the common rail is increasing, abrasive grains and stream channel wall effect is more intense, more conducive to the abrasive flow ultra-precision machining.

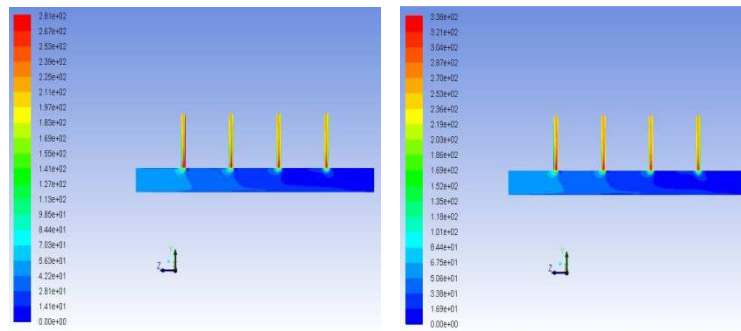
3.3 Speed Numerical Analysis

In order to better analyze the processing characteristics of the abrasive flow, to abrasive flow machining abrasive flow characteristics were numerically analyzed, the velocity vector image shown in Figure 7.



a) out of the speed of 30m / s

b) inlet velocity of 40m / s



c) out of the speed of 50m / s

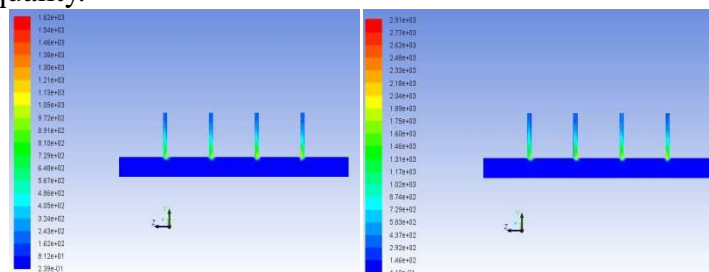
d) inlet velocity of 60m / s

Figure 7 Speed image under different conditions of entry into the speed

In the velocity vector in the direction indicated by the arrow is the direction of the moving speed, speed rail pipe holes and the hole wall trunk road junction instantaneous velocity becomes large, abrasive Flow velocity in the common rail injection hole at the maximum, you can find the speed increases with inlet pressure. From the numerical simulation results, if you want to get a larger abrasive flow machining speed should be increased inlet pressure of the workpiece. As the speed of the boundary layer and the orifice flow path difference at the surface of the orifice is increased, abrasive flow in abrasive contact with the hole wall to increase, abrasive Flow relative slip boundary between the machined surface and also increases the channel surface removal is also bigger, more conducive to the flow of abrasive finishing runner holes.

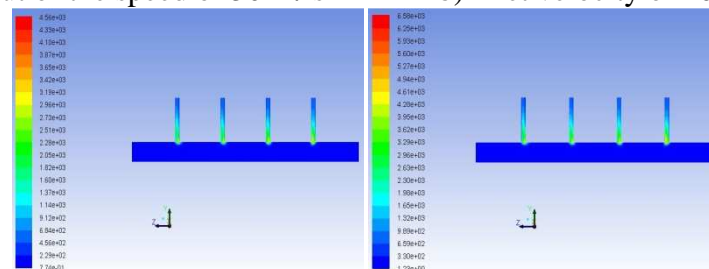
3.4 Numerical analysis of turbulent kinetic energy

Turbulent kinetic energy reflects the turbulent mixing capabilities, images from the turbulent kinetic energy can also shown in Figure 8 shows, abrasive flow holes in the common rail movement at the most intense, in the inner wall of the nozzle holes is much larger than the energy accumulated in the cell walls of the lumen flow channel turbulent kinetic energy. Therefore, abrasive flow in the common rail pipe orifice are the most active, the nozzle wall finishing stronger, in the nozzle can obtain better surface quality.



a) out of the speed of 30m / s

b) inlet velocity of 40m / s



c) out of the speed of 50m / s

d) inlet velocity of 60m / s

Figure 8 Turbulent kinetic energy image entry conditions at different speeds

From the turbulence intensity of the image shown in Figure 8, in the common rail pipe orifice of turbulence intensity is the largest, in the cross-hole turbulence intensity increased significantly, abrasive Flow hole at the intersection of the instantaneous enhancement activities. Therefore, in this part of the abrasive flow machining strongest, can guarantee precision spray holes to ensure the best performance of common rail injection tube.

4 Conclusions

From the Abrasive Flow Machining common rail passage holes numerical analysis results, use of abrasive flow machining technology fine buffing parts small hole machining is a kind of effective processing method. From the simulation results, by changing the inlet velocity of Abrasive Flow Machining obtain different results, with increasing speed, steady pressure common rail holes at the dynamic pressure, abrasive flow velocity, turbulent kinetic energy increases, abrasive cutting capacity enhancement, can obtain the desired surface accuracy. Through the common rail pipe orifice Abrasive Flow Machining process three-dimensional numerical analysis, to optimize the selection Abrasive Flow Machining parameters provide a theoretical support.

References

- [1]. Junye Li, Weina Liu, Lifeng Yang, et al. The Development of Nozzle Micro-hole Abrasive Flow Machining Equipment[J].Applied Mechanics and Materials, 2011, (44-47): 251-255.
- [2]. V.K. Jain, Rajani Kumar, P.M. Dixit, et al. Investigations into abrasive flow finishing of complex workpieces using FEM[J]. Wear, 2009, (267): 71-80.
- [3]. Liu, W.-N., Li, J.-Y., Yang, L.-F et al., "Design analysis and experimental study of common rail abrasive flow machining equipment," Advanced Science Letters, vol. 5, no. 2, pp. 576-580, 2012.
- [4]. Rajendra K J. Modeling of material removal and surface roughness in abrasive flow machining process [J]. International Journal of Machine Tools and Manufacture, 1999, 39: 1903-1923.
- [5]. Rajendra K J, Vijay K J. Optimum selection of machining conditions in abrasive flow machining using neural network [J]. Wear, 2000, 108: 62-67.
- [6]. Gorana V K, Vijay K J, Lal G K. Forces prediction during material deformation in abrasive flow machining [J]. Wear, 2006, 260:128-139.